communications earth & environment

ARTICLE

https://doi.org/10.1038/s43247-022-00568-6 OPEN

Permafrost degradation increases risk and large future costs of infrastructure on the Third Pole

Youhua Ran[1✉], Guodong Cheng[1,2], Yuanhong Dong[3], Jan Hjort[4], Amy Lauren Lovecraft[5], Shichang Kang[1], Meibao Tan[1] & Xin Li[2]

The damage to infrastructure caused by near-surface permafrost degradation is directly related to the well-being of 10 million people and the sustainable development on the Qinghai-Tibet Plateau, the Third Pole of the Earth. Here we identify the economic damage caused by permafrost degradation to infrastructure on the Qinghai-Tibet Plateau by integrating data-driven projection, multihazard index, and lifespan replacement model. We found that additional cost of approximately $6.31 billion will be needed to maintain the service function of current infrastructure under the historical scenario (SSP245) by 2090. While 20.9% of these potential costs can be saved with strategic adaptations. Controlling global warming to below 1.5 °C will reduce the costs by $1.32 billion relative to the 2 °C target of Paris Agreement. These findings highlight the importance of mitigating global warming and of investment in the adaptation and maintenance of infrastructure on the Qinghai-Tibet Plateau, which has a sparse population but is a climate hotspot.

[1] Heihe Remote Sensing Experimental Research Station, Northwest Institute of Eco-Environment and Resources, Chinese Academy of Sciences, Lanzhou 730000, China. [2] State Key Laboratory of Tibetan Plateau Earth System, Resources and Environment, Institute of Tibetan Plateau Research, Chinese Academy of Sciences, Beijing 100101, China. [3] State Key Laboratory of Road Engineering Safety and Health in Cold and High-Altitude Regions, CCCC First Highway Consultants Co., LTD, Xi'an 710075, China. [4] Geography Research Unit, University of Oulu, P.O. Box 8000, FI-90014 Oulu, Finland. [5] Center for Arctic Policy Studies, University of Alaska Fairbanks, 99775 Fairbanks, AK, USA. ✉email: ranyh@lzb.ac.cn

Warming and thawing (i.e., degradation) of near-surface permafrost can damage infrastructure by reducing substrate strength, increasing mass movement frequency and producing thermokarst activity, making it the greatest threat to infrastructure in cold regions[1–4]. Such damage shortens the lifespan of infrastructure and increases maintenance costs, leading to diverse financial risks[5]. Investments in infrastructure adaptation reduce the engineering damage rate and social inequality[6,7] and enhance social-ecosystem resilience in cold regions under a warming climate[8]. In the Northern Hemisphere, nearly 70% of the current infrastructure is at risk in areas with a high potential for degradation of near-surface permafrost by the middle of this century[3]. Current infrastructure valued at approximately $21.6 billion could be affected by permafrost degradation, which would require an additional investment of approximately $15.47 billion to maintain the service function of this infrastructure in the circumpolar Arctic by 2060[9].

The Qinghai-Tibet Plateau (QTP), a dominant part of the Third Pole, has an average altitude of 4000 m above sea level (a.s.l.) and has a developed cryosphere that is characterized by mountain glaciers, snow cover, and permafrost. Most of the Earth's permafrost in the middle and low latitudes occurs on the QTP, which is warmer than the high Arctic[10]. Nearly 40% of permafrost in the area is considered to be especially warm and unstable (ground temperature > −0.5 °C)[11,12]. Warm permafrost is especially vulnerable to climate change and ecosystem disturbances (both natural and human)[13,14].

The social and economic development of the vast QTP depends heavily on reliable infrastructure. In past decades, several economically and societally important infrastructure projects have been constructed on the QTP that focus on transportation (e.g., Qinghai-Tibet Highway, Qinghai-Tibet Railway), energy provision (e.g., Qinghai-Tibet DC power transmission line), and structures (e.g., buildings). The expansion of infrastructure has reshaped socioeconomic conditions on the QTP and the surrounding population. More than 10 million people live on the QTP, and hundreds of millions of people rely directly on this infrastructure in the form of food security, energy equality, culture, education, health care, and opportunities for sustainable development[15].

In recent decades, depending on altitude, the warming rate of the QTP has been twice the global average[16,17]. Warm permafrost associated with pronounced warming can lead to higher degradation potential than that in other permafrost areas[3,18,19]. Climate change-induced permafrost degradation can seriously threaten the stability of infrastructure on the QTP[20,21]. Many adaptation measures have been developed and applied to adapt to the stressors from permafrost degradation and reduce the engineering damage rate. For instance, several proactive roadbed cooling engineering measures, such as shading boards, ventilation ducts, thermosyphons, and air-cooled and crushed rock embankments, have been successfully applied in the Qinghai-Tibet railway and highway[22,23]. Thermosiphons, fibreglass-reinforced plastic coverings, and excavated and pile foundations have been applied along the Qinghai–Tibet Power Transmission Line[24]. However, previous permafrost studies on the QTP have mainly focused on biophysical changes, ignoring permafrost vulnerability and impact, especially economic impact, which is critically important for social decision-making[25]. It is still unclear how much infrastructure on the QTP will be vulnerable to permafrost degradation in the future. The uncertainty of cost increases and technological development make it impossible to plan engineering adaptation measures that are most economical at the regional scale. Considering the rapidity of permafrost degradation, it is important to project the effects of permafrost degradation and assess the financial investment of targeted adaptation strategies for infrastructure protection.

In this study, we quantified the future risk of current infrastructure (including major roads, railways, powerlines, and buildings) exposure to permafrost degradation and its additional costs, defined as the difference in net present value for infrastructure replacement over time under the normal case (no permafrost degradation) and under permafrost degradation with and without adaptation on the QTP under four shared socioeconomic pathways (SSP126, SSP245, SSP370, and SSP585) and two global warming (1.5 °C, 2.0 °C above preindustrial levels by the end of this century) conditions in the Paris Agreement (see Methods). A well-trained ensemble statistical/machine learning model was used to project the mean annual ground temperature (MAGT) and active layer thickness (ALT) for the reference period in 2008 (2000–2016) and future periods in 2050 (2040–2060) and 2090 (2080–2100) with a 1 km resolution. A consensus of five hazard indices was used to quantify the potential hazard level of future permafrost degradation. Then, a lifespan replacement model was used to quantify the future cost of the current infrastructure caused by permafrost degradation with and without adaptation. A simplified damage relationship between the potential hazard level of permafrost degradation and the equivalent lifespan of infrastructure was used to parameterize the lifespan replacement model.

Our results demonstrate that approximately 63.3% of the permafrost area will be located in a high-hazard zone under the historical climate scenario (SSP245) by 2090. Correspondingly, approximately 60% of the current infrastructure in the permafrost area will be exposed in the high-hazard zone, and an additional cost of approximately $6.31 billion will be needed to maintain the service functions of the current infrastructure without adaptation measures. However, 20.9% of the potential additional cost can be saved through strategic adaptation measures by 2090. An additional cost of approximately $5.65 billion will be needed, even if the Paris Agreement target (global warming of 2.0 °C) is achieved.

Results

Projected changes in permafrost thermal state. The simulated results showed that the area of permafrost extent on the QTP was approximately 101×10^4 km^2, and the average MAGT at a depth of zero annual amplitude (10–25 m) and ALT were −1.72 (−2.23 to −1.30) °C and 2.11 (1.75–2.48) m, respectively, for the reference period in 2008 (2000–2016). The average MAGT over the QTP was projected to increase by 1.55 °C in 2050 (2041–2060) under SSP245 and to further increase by 0.82 °C by the end of this century, i.e., 2090 (2081–2100) (Supplementary Table 1). The average ALT was projected to increase by 0.62 m from the reference period to 2050 (2041–2060) (SSP245) and further increase by 0.26 m by the end of this century. Consistent with the change in MAGT, ALT will increase by 1.61 m under SSP585 (rapid and unconstrained growth scenario) from the reference period to 2090 (2081–2100). Controlling global warming below 1.5 °C may reduce permafrost warming by 0.75 °C relative to the 2 °C target.

The fine-resolution projection suggests that there will be substantial but region-specific changes in MAGT and ALT due to climate change in this century (Supplementary Figure 2). The increase in the average MAGT in the western and southern QTP was generally greater than 1.5 °C from the reference period to 2050 (2041–2060) (SSP245). It was significantly larger than that in the eastern and northern QTP, whereas the corresponding increase was approximately 1.2 °C. The pattern of the ALT change was generally consistent with the change in MAGT. For the areas within 10 km of the Qinghai-Tibet Railway from Golmud to Lhasa, the most important engineering corridor on the QTP, the corresponding increase in average MAGT was approximately 1.36 °C (the ALT increased by 0.64 m) from the

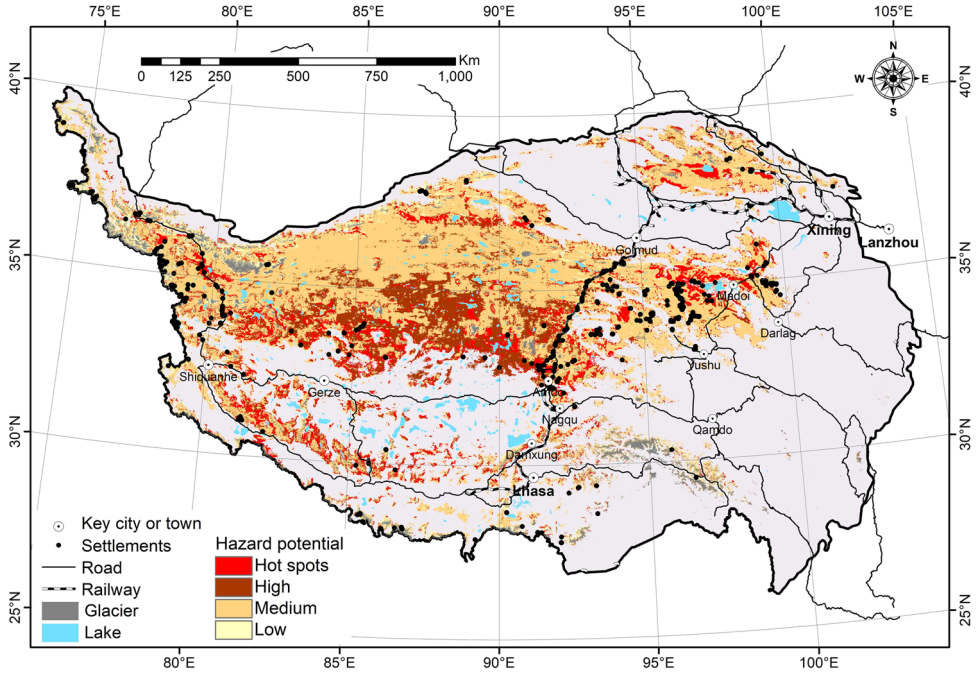

Fig. 1 The distribution of infrastructure hazard zones by 2050 (2041-2060) under the historical scenario (SSP245). The hazard levels (high, medium and low) of permafrost degradation for infrastructure were derived from five hazard indices (thermal index, settlement index, bearing capacity index, risk zone index, and expert-based index) using a majority vote procedure. Hotspot areas indicate that at least four indices showed high hazard levels. Infrastructure, including backbone road networks, railways, and buildings, is shown, while the distribution of power lines is generally consistent with the road network. Thus, the infrastructure pattern over the Qinghai-Tibet Plateau mainly includes three regions, i.e., the western engineering corridor (north of Shiquanhe), the central Qinghai-Tibet engineering corridor from Golmud to Lhasa, and the eastern corridor around Madoi. The infrastructure distribution data extracts from OpenStreetMap data and are licensed under CC BY-SA 2.0 (https://creativecommons.org/licenses/by-sa/2.0/). Glacier and lake extent data obtained from National Tibetan Plateau Data Center (10.3972/glacier.001.2013.db) and are licensed under CC BY 4.0 (https://creativecommons.org/licenses/by/4.0/).

reference period to 2050 (SSP245) and increased by another 1.83 °C (ALT increased by 0.96 m) by the end of this century. This warming rate is generally consistent with historical measurement data[19]. The near synchronous warming of permafrost with near-surface air temperature on the QTP is probably due to the weak surface thermal offset of sparse vegetation, dry soil, thin snow cover, and low organic matter content and is thus climate-driven[14].

Permafrost degradation can lead to subsequent hazards that threaten engineering infrastructure through the complex interaction of multiple physical processes, including mechanical processes such as loss of foundation bearing capacity and ground subsidence associated with the phase change of pore water and ground ice in the permafrost, thermal processes such as the development of talik and thermokarst, and mass wasting processes on slopes[2]. This process of degradation may affect the service function of infrastructure and thus increase the infrastructure repair and replacement frequency. The consequence can be expressed as the shortening of useful life and is closely related to hazard levels.

Trends in the hazard level of permafrost. Associated with the warming of permafrost and the thickening of the active layer, the hazard level of permafrost on the QTP is rising, but there are significant differences among SSPs. By 2050, the proportion of infrastructure in high-hazard zones is predicted to be approximately 28.66 (7.78–52.35)% under SSP245 (Fig. 1) but will increase to 63.25 (23.25–78.70)% under SSP585 by 2050 and further increase to 83.52 (73.85–95.46)% by the end of this century. Accordingly, the areas of medium and low hazard will decrease (Supplementary Table 2). However, the proportion of infrastructure in high-hazard zones is predicted to be approximately 17.62 (5.83–26.13)% under SSP126 (the green scenario) by 2050, which is significantly smaller than those under other SSPs. Regionally, the high-hazard hotspot areas are mainly distributed in the source area of the Yellow River, the Qinghai-Tibet engineering corridor, and the Xinjiang-Tibet highway corridor (Fig. 1), where the infrastructure is relatively concentrated and may be critically damaged.

Infrastructure in the high-hazard zone. Currently, more than 9,389 km of roads, 580 km of railways, 2,631 km of power lines, and 1,064,590 m^2 of buildings are located in the QTP permafrost area. This infrastructure may be affected by the increasing hazard level of permafrost in the future. By 2050, 38.14% (19.92–60.36%) of roads, 38.76% (11.35–71.30%) of railways, 39.41% (14.82–31.28%) of power lines, and 20.94% (14.82–31.28%) of buildings may be threatened by permafrost degradation in high-hazard areas (SSP245) (Fig. 2a, Supplementary Table 3). These proportions may nearly double over the decades following 2050 (Supplementary Figure 3). The global climate warming goals of the Paris Agreement, i.e., to limit warming to well below 2 °C above preindustrial levels, preferably to 1.5 °C, could have a considerably different influences on infrastructure hazards by the end of this century (Fig. 2b). Controlling global warming below 1.5 °C may reduce the infrastructure in high-hazard zones by approximately half relative to the results under the 2 °C target.

Additional costs to maintain the service function of the current infrastructure. The lifespan of infrastructure will be significantly reduced due to damage from permafrost degradation. The degree of damage is related to the hazard level of permafrost. Long-term

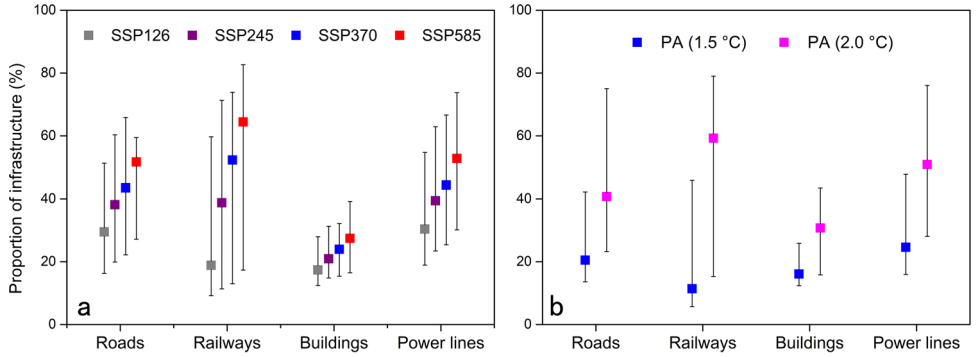

Fig. 2 The proportion of current infrastructure in the high-hazard zone under different scenarios. The mean value (square) with uncertainty ranges (bars) by 2050 (2041–2060) under four shared socioeconomic pathways (SSPs) (a) and the target of the Paris Agreement (PA) by the end of this century (b). The uncertainty ranges (bars) were based on the ranges of the mean annual ground temperature and active layer thickness predictions, quantified using the 97.5th and 2.5th percentiles of the ensemble predicted mean annual ground temperature and active layer thickness with 200 runs.

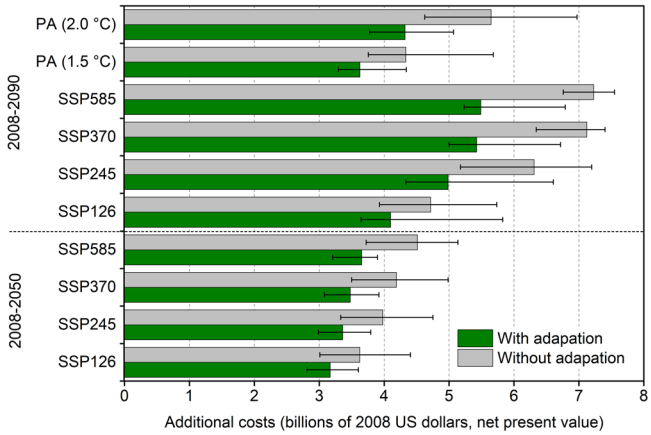

Fig. 3 Additional infrastructure costs from permafrost degradation under different scenarios. Cumulative additional costs during reference period and projected periods, net present value in 2008 billions of US dollars, 2.85% discount rate. The uncertainty ranges were based on the ranges of the mean annual ground temperature and active layer thickness predictions, quantified by using the 97.5th and 2.5th percentiles of the ensemble predicted mean annual ground temperature and active layer thickness with 200 runs.

observation data for the Qinghai-Tibet Highway over the past 60 years show that the lifespan of the road may be reduced by more than 50% in high-hazard areas[26]. This change will lead to a substantial increase in costs due to the damaged infrastructure that needs to be repaired, possibly relocated, or completely replaced to maintain its service function[27].

Our assessment shows that significant additional costs will be required to maintain the service function of the current infrastructure. From 2008 (reference period) to 2050, the additional cost of $3.98 (3.33–4.75) billion (net present value, 2.85% annual discount rate) will be needed to cover the costs of permafrost degradation under SSP245 (Fig. 3). The transportation infrastructure includes roads and railways that account for most of the costs, i.e., 93% (87% for roads, 6% for railways) (Supplementary Table 4). Other infrastructure includes power lines and buildings, which account for 7%. Under SSP126 (the green scenario), an additional cost of $3.62 (3.01–4.44) billion will be required by 2050, which is a substantial reduction of $0.35 billion compared to the results under SSP245. This reduction could further increase to $1.59 billion by 2090. The adaptation measures for highways (and paved roads), railways, power lines and buildings would greatly reduce this additional cost (the cost of adaptation measures has been deducted, see Methods) (Fig. 3). By 2050, the percentage of potential cost savings from adaptations is approximately 15.36% (SSP245). This savings could reach 21% by the end of the century. For low-grade roads or high-grade roads in low-risk areas, additional adaptation measures may be less economical (i.e., the cost of adaptation measures is greater than the reduction of maintenance costs), so they were excluded from this analysis. The impact of the global warming goals of the Paris Agreement (2.0 °C or 1.5 °C) on these additional costs is also considerable. Controlling global warming below 1.5 °C may save $1.32 billion relative to the costs under the 2 °C target by the end of the century.

Distribution of additional costs over the Qinghai-Tibet Plateau. The distribution of cumulative additional infrastructure costs during this century varied across the prefectural-level regions over the QTP (Fig. 4a, b). Under the SSP585 scenario, the highest additional costs were projected in the central-eastern regions, including Yushu, Golog, Haixi, and Nagqu, while the lowest additional costs were projected in the northern and southeastern prefectures, including Bayingolin, Lhasa, Linzhi, Qamdo, and Garze (Fig. 4b), due to the small proportion of permafrost or small infrastructure inventory in those areas. Almost all prefectures in permafrost regions will need additional investment in infrastructure, but the investment will be lower under SSP245 than under SSP585 (Fig. 4a, b), indicating the benefits of low carbon development at the global scale on the QTP. The largest reductions in the per capita additional costs between SSP245 and SSP585 were projected in Golog and Yushu (Fig. 4c, d). In both the SSP245 or SSP585 scenarios, the additional investment in Ngari is very important because it is a low-cost corridor relative to the Qinghai-Tibet engineering corridor, which helps to enhance the connectivity between the Qinghai-Tibet Plateau and the surrounding area and thus to enhance the social resilience of the Qinghai-Tibet Plateau.

Discussion

Based on the data-driven or knowledge-informed data-driven projection of permafrost thermal degradation, this study quantified the hazard potential of permafrost degradation, its associated effect on current infrastructure and its future additional maintenance costs with and without adaptation. We found that the near-surface permafrost on the QTP warmed nearly synchronously with the air temperature. A high proportion of infrastructure will be exposed in areas with rapid warming associated with permafrost with high hazard potential. Thus, permafrost

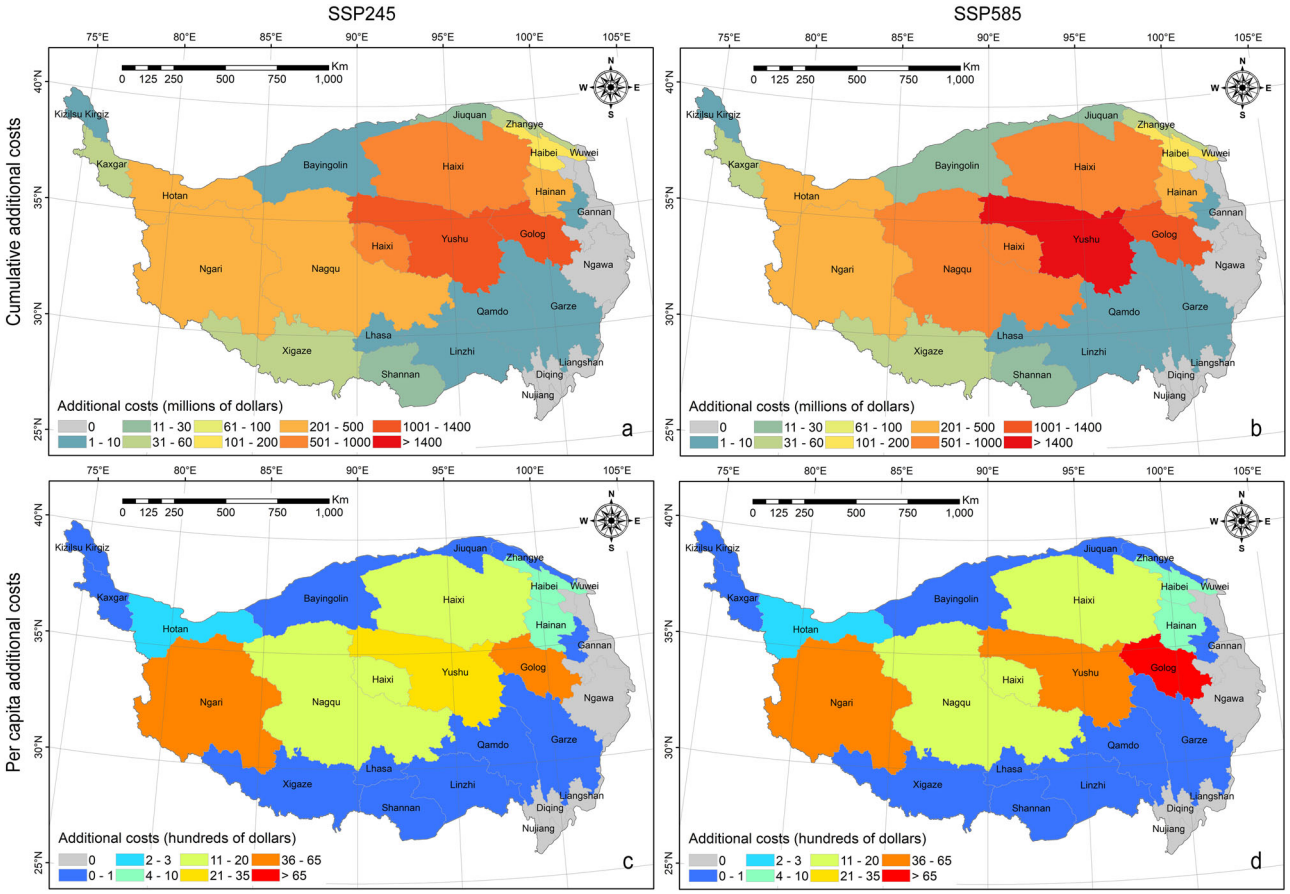

Fig. 4 Distribution of additional costs of current infrastructure with adaptation from permafrost degradation across the Qinghai-Tibet Plateau. Cumulative additional costs (2008–2090; net present value in 2008 US dollars, 2.85% annual discount rate) (**a, b**) and per capita additional costs (**c, d**) estimates for each prefectural-level city under SSP245 (**a, c**) and SSP585 (**b, d**). The population data used to calculate the per capita additional cost came from the sixth national census of China in 2010. Boundary of prefectural-level city dataset is from National catalogue Service for Geographic Information (www.webmap.cn) and licensed under CC BY 1.0 (https://creativecommons.org/licenses/by/1.0/).

degradation increases the risk to and future costs of infrastructure on the QTP even under the green scenario (SSP126) and when controlling global warming below 1.5 °C by the end of the century.

Sustainable regional planning and highly resilient infrastructure management require information on the costs of maintaining construction under climate change[9,28–30]. Economic damage information from climate change is also critically important for understanding the benefits of social investments for reducing greenhouse gas emissions and climate mitigation[25]. This information is available for Alaska[1,27], Canada[31] and Russia[32–35]. For example, the costs of permafrost damage to Alaska's public infrastructure were estimated to be $1.6 billion for representative concentration pathway (RCP) 4.5 by the end of this century[1]. In Russia, the total cost of support and maintenance of road and building infrastructure due to permafrost degradation from 2020 to 2050 could be as high as $34 billion[33,34]. However, these central estimates are lacking for the QTP, which is the largest permafrost region in the middle and low latitudes of the world.

This study found that the amount of infrastructure in the QTP permafrost area is less than that in Alaska[27], but its economic damage is much larger[1]. However, this value is much lower than that in Russia[30,33,34], where the amount of infrastructure is much greater than that on the QTP due to Russia's vast area. The larger economic damage on the QTP than in Alaska is probably due to the higher degradation rate of warm, arid and climate-driven permafrost on the QTP[14] and the different infrastructure components, and the methods include permafrost projection, stressor–response relationships, and spatial resolution. The damage caused by permafrost degradation in Alaska[1] represented only the cost required for infrastructure replacement. It also distinguished the damage caused by permafrost degradation due to flooding, precipitation, and freeze-thaw cycles. In this study, because permafrost degradation is driven by climate change and closely related to air temperature, precipitation, freeze-thaw cycles, and even flooding[36,37], infrastructure damage is difficult to separate from these related factors. Therefore, the damage considered in this study is the apparent damage associated with permafrost degradation. Considering this inherent difference, the economic damage estimation in this paper is comparable to that in Melvin et al. (2017) but smaller than the estimation of Larsen et al. (2008).

The large additional costs of infrastructure damaged by permafrost degradation on the QTP provide insights in at least two ways. First, adaptation measures (e.g., shading boards, ventilation ducts, thermosiphons, air-cooled and crushed rock embankments for roads and railways; gravel pads for buildings, thermosiphons, fibreglass-reinforced plastic covering, and excavated and pile foundations for power line towers) are generally economical options to increase infrastructure stability at the regional scale. Compared to no adaptation, the proportion of additional cost saved by taking adaptation measures ranges from 12% (SSP126 by 2050, $0.45 billion) to nearly 24% (SSP585 by 2090, $1.74 billion) (Table 1). The benefit of adaptation increases with an increasing warming rate and analysis period. However, it is likely that a

Table 1 Additional costs from permafrost degradation under future scenarios over the Third Pole. The scenarios including four shared socioeconomic pathways (SSPs) and two Paris Agreement (PA) targets. Additional costs is present value in 2008 (billions of US dollars, 2.85% discount rate).

Projected periods	Normal (No permafrost degradation)	Adaptation	SSP126	SSP245	SSP370	SSP585	PA1.5	PA2.0	Potential savings from adaptations
2008-2050	9.16	No	3.62	3.98	4.19	4.51	-	-	
		Yes	3.17	3.36	3.48	3.65	-	-	12-19%
2008-2090	11.70	No	4.72	6.31	7.12	7.23	4.33	5.65	
		Yes	4.1	4.99	5.42	5.49	3.63	4.32	13-24%

Table 2 The infrastructure database in the permafrost region of the Third Pole.

Type of infrastructure	Subtype	Length/area	Useful life (years)	Replacement cost per unit (in 2008 US dollar)	Units	Additional adaptation cost (% of replacement cost)
Roads	Grade 1	274 km	20	6.52 million	Per km	10%
	Grade 2	769 km	20	2.9 million	Per km	19%
	Grade 3	1227 km	15	0.72 million	Per km	30%
	Grade 4	2257 km	10	0.14 million	Per km	50%
	Other	4862 km	10	0.04 million	Per km	50%
Railway		580 km	100	3.62 million	Per km	20%
Building	Residential	1,064,590 m^2	50	290	Per m^2	5%
Power line	Lines network and Tower	2631 km	15	0.1 million	Per km	5%

deficit would occur (i.e., the increased cost from adaptation is less than that caused by the reduction of replacement costs due to increased lifespan) for low-grade roads (grade 4 and other roads) when adopting measures under all SSPs unless the ratio of the adaptation cost to the construction cost is greatly reduced to the level of high-grade highways in the future. This result is consistent with engineering practices in which adaptive measures are rarely used in low-grade roads. Thus, the damage relationship between the permafrost hazard level and economic loss used in this study is reasonable. Second, the damage is significantly different among socioeconomic development pathways and warming targets. By 2050, compared to the historical scenario (SSP245), the weak mitigation scenario (SSP370) may place an additional nearly 19% of the current infrastructure at high risk, and the corresponding economic damage would increase by nearly 5% ($0.21 billion without adaptation). This proportion may further increase to more than 40% (13%, $0.53 billion) under the rapid and unconstrained growth scenario (SSP585), while the proportion would decrease by 29% (9%, $0.36 billion) under the green scenario (SSP126). By the end of this century, the differences become greater (Supplementary Table 3, Table 4, Supplementary Figure 4). If global warming is controlled to below 1.5 °C by the end of this century, the quantity of high-risk infrastructure will be nearly 57% less than that under the 2 °C target, and the corresponding additional cost will be reduced by approximately 23% ($1.32 billion without adaptation). This difference highlights the importance of global green development and reducing greenhouse gas emissions to the vulnerability of infrastructure on the QTP. Additionally, the maintenance/repair of roads in permafrost areas is generally much more expensive than normal maintenance in nonpermafrost areas, reaching a more than 8-fold difference in some cases[38]. The high infrastructure maintenance cost in permafrost areas combined with the amplification effect of warming[16,39] may lead to a more negative consequence of climate change on the QTP and thus exacerbate potential social inequality[6]. Increasing infrastructure investment, the development of less expensive adoption technologies, and a global coordinated green development policy would help to reduce exposure and to enhance the stability of vulnerable infrastructure and safety, thus reducing this social inequality on the QTP.

Quantifying the impact of permafrost degradation on infrastructure at the regional scale is very challenging due to the complex process of damage and the gap between regional and local scales[5]. The uncertainty of the estimated additional costs is substantial but probably conservative and mainly comes from the following aspects: the projected permafrost thermal state, the infrastructure database, the damage relationship between the potential hazard level of permafrost and economic loss, and the inherent limitations of the equivalent lifespan replacement model. First, for the projection of the permafrost thermal state, it should be feasible to simulate future changes in permafrost temperature and active layer thickness based on climate-dominated predictors (see Methods) because permafrost changes over the QTP are primarily climate driven[14]. However, the statistical/machine learning model based on the large-scale models (i.e., the simplified Stefan equation used in this study) cannot resolve the relatively local process, such as talik, that are usually considered nonlinear and ecosystem driven[40,41]. The thermal state of permafrost is also significantly affected by local disturbances, especially in the eastern part of the QTP, where the permafrost is modified by ecosystem conditions. The absence of the local process may lead to underestimated potential hazards. However, this underestimation may be partially offset by the latent heat process. That is, as the permafrost temperature approaches the phase transition value, the latent heat process may slow the warming rate of permafrost and propagate to the hazard level via the MAGT-based thermal index. However, this process may slow the disappearance of permafrost, but its hazard level is still high due to talik formation beneath engineering facilities under warming conditions. Thus, the net effect of the estimated additional costs is considered conservative. Second, for the infrastructure database (Table 2), the available replacement cost information under warming conditions is very scarce and generally not available because the data are sometimes cross-departmental, sensitive, and confidential. This study collected information mainly from planning and design materials, previous

studies, and personal communications with relevant employees and academic researchers in related fields. Thus, the data and information from different sources may contain some uncertainties. Additionally, more infrastructure will be built in the future. From this point of view, the projection of the additional costs in the future is conservative. Third, we assigned the potential reduction in the utilization lifespan of infrastructure due to permafrost degradation based on observational evidence for the Qinghai-Tibet Highway over the past 60 years[26] and personal empirical judgement with the assistance of relevant employees in related industries (Table 2). The infrastructure over the QTP is dominated by roads. Therefore, direct evidence of highway damage ensures the objectivity of the projection and credible trend analysis. Here, we quantified the uncertainty of the hazard level and corresponding affected infrastructure by using the 97.5th and 2.5th percentiles of the ensemble simulated MAGT and ALT with 200 runs. Five geohazard indices were combined to reduce the uncertainty of a single index. Considering this uncertainty and the conservative scheme, the quantity and additional cost of infrastructure potentially affected by permafrost degradation are probably not considerably smaller (Figs. 2, 3). However, this kind of rough estimation at the regional scale may be different from the fine-scale analysis in the engineering field based on a very detailed classification of materials and construction processes, but the trend should be mostly consistent. To bridge the gap between regional and engineering scales, more data are required to support precise estimation. Finally, for the lifespan replacement model, the simplified annual replacement costs (i.e., the replacement costs divided by useful life) used in the equivalent lifespan replacement model to calculate the present value over a chosen time horizon make the present value under permafrost degradation conditions that are sensitive to the chosen calculation horizon. This effect occurs because the future replacement costs at the end of the (adjusted) useful life are not treated as a future value (and are not discounted). This limitation and the low real discount rate (i.e., 2.85%) used in this study would lead to less total discounted costs both for normal and permafrost degradation conditions, although this has little impact on the results of additional costs because the effects under the two conditions offset each other. This inherent limitation of the model needs to be improved in the future by deeply integrating the process with engineering economics.

The vulnerability of infrastructure on the QTP associated with the fragility of social–ecosystem interactions highlights the need for investment in the adaptation and maintenance of infrastructure for sustainable development on the QTP and the surrounding areas. This study provides quantitative information on the additional economic costs and benefits of technological adaptation and global green development of QTP infrastructure. The ultimate investment may be potentially much higher than the conservative and preliminary estimates, depending on future technological, social and economic development and the global socioeconomic pathways.

Materials and methods

The exposure and risk of the current infrastructure and its future additional costs caused by permafrost degradation were evaluated by integrating a statistical/machine learning model-based ensemble projection, multihazard index, and lifespan replacement model (Supplementary Figure 1). First, based on the MAGT at a depth of zero annual amplitude (10–25 m) and ALT measurements (253 MAGT boreholes and 157 ALT sites) during 2000–2016 (Supplementary Figure 2)[10], a well-trained ensemble statistical/machine learning model was used to predict the MAGT and ALT for the reference period in 2008 (2000–2016) and future projections in 2050 (2040–2060) and 2090 (2080–2100) with a 1 km resolution. The downscaled and bias-corrected climate model output, i.e., WorldClim (https://worldclim.org)[42], under four shared socioeconomic pathways (SSPs), i.e., green scenario (SSP126), historical scenario (SSP245), weak mitigation scenario (SSP370), and rapid and unconstrained growth scenario (SSP585), and two global warming (1.5 °C, 2.0 °C above preindustrial levels by the end of this century) conditions outlined in the Paris Agreement were used as climate predictor variables together with soil and terrain variables. Second, a consensus of five hazard indices was developed based on the simulated MAGT and ALT and other environmental factors to identify the potential hazard level of permafrost degradation. Finally, a lifespan replacement model was used to quantify the future cost to current infrastructure caused by permafrost degradation with and without adaptation measures based on an infrastructure database and the potential hazard level of permafrost degradation. A simplified damage relationship between the potential hazard level and the useful life of infrastructure was used to parameterize the lifespan replacement model.

Projection of ground temperature and active layer thickness. MAGT was projected based on an ensemble mean of five statistical/machine learning models (GLM: generalized linear model; GAM: generalized additive model; SVR: support vector regression; RF: random forest; GWR: geographically weighted regression)[12]. A distance-blocked (3000 m) resampling training dataset with 200 repetitions was used by relating the in situ measurement with eight predictor variables. These variables included the freezing degree-days and thawing degree-days (i.e., the annual degree-day totals below and above 0 °C, respectively), solid precipitation ($T \le 0$ °C), liquid precipitation ($T > 0$ °C), soil bulk density, soil organic content, solar radiation, and elevation. The uncertainty ranges of the MAGT and ALT predictions quantified using the 97.5th and 2.5th percentiles of the ensemble results with 200 runs. A 10-fold cross-validation showed that the acceptable accuracy of MAGT (RMSE = 0.93 °C, bias = −0.02 °C) was achieved.

The ALT was estimated using the simplified Stefan equation[40]:

$$ALT = E\sqrt{TDD} \quad (1)$$

where TDD is thawing degree-days, E is a scaling parameter (E-factor) influenced by local characteristics, including vegetation, snow cover, and local soil texture. The E-factor was estimated based on an ensemble mean of five statistical/machine learning models based on the E-factor apparent measurement at 157 sites for the baseline, and it remained constant in the future periods. Although the E-factor may change with the change in vegetation and snow cover in the future, the effect of vegetation and snow cover on permafrost is small due to the low snow cover, arid climate, and sparse vegetation on the QTP. Compared with the simulation error level of ALT itself, the error caused by the constant E-factor is ignored here[43].

A 10-fold cross-validation showed an acceptable accuracy of the E-factor (RMSE=18.7, bias=−0.05).

The freezing degree-days, thawing degree-days, solid precipitation, and liquid precipitation were recalculated based on the downscaled and bias-corrected monthly temperature and precipitation data, i.e., WorldClim version 2.1 (https://worldclim.org)[42]. Following ref. [44], the WorldClim climate data for 1970–2000 were temporally adjusted to the reference period in 2008 (2000–2016) using the locally smoothed (3×3 pixels) difference between the 2.5-minute WorldClim weather data and the WorldClim climate data. For future periods, i.e., 2050 (2040–2060) and 2090 (2080–2100), the downscaled climate projections from WorldClim, including monthly mean temperature and precipitation, were derived from eight downscaled General Circulation Model outputs of Coupled Model Intercomparison Project phase 6 for four SSPs (126, 245, 370, and 585) with a 0.05° resolution but adjusted to a 1 km resolution using the locally smoothed (3×3 pixels) difference between the SSPs and downscaled Coupled Model Intercomparison Project phase 5 data for 2070 with a 1 km resolution. For the two global warming scenarios, following ref. [45], the mean WorldClim climate data from eleven downscaled General Circulation Model outputs of Coupled Model Intercomparison Project phase 5 for 2061–2080 under RCP2.6 were used for the 1.5 °C global warming condition, and those under RCP4.5 for 2061–2080 were used for the 2.0 °C global warming condition. The soil bulk density, soil organic content, and two terrain-related factors were considered to be unchanged in future periods. The soil bulk density (kg m − 3) and soil organic content (g kg−1) were derived from global SoilGrids250 datasets (https://soilgrids.org)[46]. Solar radiation (kJ m-2 day-1) data derived from WorldClim version 2.1 and the NASA Shuttle Radar Topography Mission digital elevation model at a 30 arc-second spatial resolution were used.

Identification of the potential hazard level. Several indices have been developed to evaluate the potential hazard level of permafrost degradation. In this study, to reduce the uncertainty of a single index, a composite index was used to identify the hazard level (high, medium and low) of permafrost degradation that integrated the thermal index (I_t), settlement index (Is), bearing capacity index (I_b), risk zone index (I_r), and expert-based index (I_a) with surface conditions. The five indices were defined and produced as follows.

First, the thermal index (I_t) was represented by the relative change in MAGT, which is one of the most direct and reliable indicators for permafrost occurrence and is closely related to bearing capacity and permafrost distress[47,48]. Following the altitude permafrost classification system for the QTP[12] and embankment distress characteristics with varying MAGT[26], we classified the permafrost into three types: cold (<−3.0 °C), cool (−1.5 to −3.0 °C), and warm (0 to −1.5 °C). The type transitions during the baseline period and future conditions were used to determine the hazard level (permafrost disappearance or change from cold to warm=high, cold to cool or cool to warm=medium, no type transition=low)[1,3].

Table 3 The reduced proportion of the useful life of infrastructure due to permafrost degradation.

Hazard level	Reduction of useful life	
	Without adaptation	With adaptation
High	40%	20%
Medium	25%	10%
Low	15%	5%

The proportion is determined according to a long-term investigation of maintenance history, permafrost-related distress to the foundation, and adaptation effect of the roads in Qinghai-Tibet over the past 60 years, communication with local experts, and previous research. We assume that adaptation measures extend useful life but vary among different hazard levels. This proportion may be different in different types and even subtypes of infrastructure, but these data are not available; therefore, we assumed the proportion to be consistent across types here.

Second, the settlement index (I_s)[17] was calculated as follows:

$$I_s = \Delta\mathrm{ALT} \times V_{ice} \tag{2}$$

where ΔALT is the relative increase in ALT and V_{ice} is the volumetric proportion of excess ground ice. Ground ice content data with a 1 km resolution estimated based on 164 borehole measurement data and a map of Quaternary sedimentary type over the QTP were used in this study[49]. Following ref. [3], class-specific values (5, 15 and 35%) were assigned, and the I_s values were reclassified into three classes using a nested means procedure[50] with the two lower classes combined for a conservative estimate.

Third, the bearing capacity index (I_b) was represented by the relative change in allowable bearing capacity. Bearing capacity was computed using a linear statistical model[47] that varied among different soil texture types based on laboratory measurements, but only two soil types were used, which were limited by soil data. The two soil groups were derived from a weighted dominant soil texture class of SoilGrids 1 km data according to coarse and fine sediments (fine=silt and finer class, coarse=sand and coarser class).

$$I_b = \begin{cases} -0.3339 \times \mathrm{MAGT} + 0.4659, & \text{for coarse class} \\ -0.1979 \times \mathrm{MAGT} + 0.3046, & \text{for fine class} \end{cases} \tag{3}$$

The resulting I_b values were reclassified into three classes using a nested means procedure.

Fourth, the risk zone index (I_r)[51,52] was developed based on a multilevel decision flow diagram by combining the surface condition, soil grain size, ice content, and permafrost thaw potential. First, the SoilGrids 250 m absolute depth to bedrock (cm)[46] was used to determine exposed bedrock areas that were directly assigned to the low hazard level[51]. The soil grain size groups were derived from a weighted dominant soil texture class of SoilGrids 1 km data according to coarse and fine sediments (fine=silt and finer class, coarse=sand and coarser class). A ground ice content with a 1 km resolution[49] was used to determine areas of high (>20%) and low (≤20%) ground ice content. The thaw potential of permafrost was defined based on the simulated MAGT (high potential=permafrost thaw; low potential=permafrost remaining).

Fifth, the expert-based index (I_a) was produced using multicriteria decision-making by integrating the relative increase in ALT and MAGT, ground ice content, fine-grained soil content, and slope gradient. All of these criteria were first classified into three classes. For MAGT, the thermal index was used. The original range classes (≤10%, 10–20%, and >20%) of ground ice content were reclassified into three value-specific classes (5, 15 and 35%). The relative increases in ALT, fine-grained sediment, and slope criterion were reclassified using the nested-means approach. The weight coefficients sourced from Hjort et al. (2018)[3] were determined based on the analytic hierarchy process.

$$I_a = 0.525 \times \Delta\mathrm{MAGT} + 0.248 \times V_{ice} + 0.122 \times \Delta\mathrm{ALT} + 0.071 \times \text{fine soil content} + 0.035 \times \text{slope gradient} \tag{4}$$

The five indices were combined using a majority vote procedure based on ArcMap's cell statistics tool to represent the potential hazard level of permafrost degradation. In draw situations, i.e., a value had the same number of votes (for example, 2 high hazard vs. 2 low hazard votes, 1 moderate hazard), a moderate hazard level was forced manually. As a result, the high-hazard zone comprised 63.3%, the medium-hazard zone comprised 34.7%, and the low-hazard zone comprised 2% of the study area under the historical scenario (SSP245) for 2090 (2081–2100). The proportions of high-hazard zones, medium-hazard zones, and low-hazard zones were 16.9%, 71%, and 12.1%, respectively, under the green scenario (SSP126) for 2090 (2081–2100).

The uncertainty range of the hazard level corresponding to the uncertainty of the projected MAGT and ALT was also calculated. This uncertainty range will affect the statistics of infrastructure distribution at different hazard levels and ultimately affect the cost calculation.

Lifespan replacement model. The additional costs of current infrastructure in the future caused by permafrost degradation were assessed using an equivalent lifespan replacement model proposed by Larsen et al. (2008)[27] that was improved to allow the calculation of the net present value (PV) of infrastructure economic damage by combining the potential hazard level of permafrost degradation with the equivalent lifespan of infrastructure. This value is based on the assumption that a reduction in the lifespan of infrastructure caused by permafrost degradation leads to higher costs due to the impacted infrastructure that needs to be repaired, relocated, completely replaced more frequently or adapted to the built environment to maintain its service function[27]. The relationship between the potential hazard level and lifespan of infrastructure is more direct than that of temperature and precipitation in the original model. The equivalent lifespan replacement model is characterized by a clear structure and is easy to understand and has been successfully applied to the economic damage assessment of infrastructure caused by climate change in Alaska and Russia. The additional costs (Φ) are computed as the cost difference under the conditions between permafrost degradation and the normal case:

$$\Phi = PV_{Permafrostdegradation} - PV_{normal} \tag{5}$$

$$PV_{normal} = \sum_{j}^{8} \sum_{i=2008}^{2050\,or\,2090} \frac{L_j RC_j}{UL_j (1+r)^{i-2008}} \tag{6}$$

$$PV_{Permafrostdegradation} = \sum_{j}^{8} \sum_{h=1}^{3} \sum_{i=2008}^{2050\,or\,2090} \frac{L_j RC_j}{AUL_{hj} (1+r)^{i-2008}} \tag{7}$$

where j is the infrastructure type, h is the potential hazard level, L is the quantity (length or area) of the corresponding infrastructure type, r is the real discount rate and 2.85% is used in this study following ref. [27], which is low but reflects the current situation for evaluating the costs of public infrastructure with public funds. RC is the replacement cost per unit. UL is the normal case useful life (Table 2), and AUL is the adjusted useful life related to the permafrost hazard level (h) and whether adaptation measures have been taken (Table 3). Here, we assume that the UL and AUL are constants (it is possible that these values are variable under accelerated climate change, but we have not identified such changes in this initial work as we are limited by the knowledge gap). The adjusted useful life is determined based on a long-term investigation of maintenance history, permafrost-related foundation distress, and adaptation effects of the road along Qinghai-Tibet over the past 60 years[26], communication with local experts, and previous research[1,9,27]. Investigation shows that an increase of 0.5 °C in MAGT would induce a decrease in the average service life for highways of more than 4 years (nearly 40%/°C and 60% for high hazard levels). This value is finally adjusted mainly in accordance with the design life and component of construction cost based on the assumption that the subgrade would not require complete reconstruction and that reconstruction would not be as expensive as initial construction. If an adaptation measure was adopted, increases in useful life and cost were both incurred. For roads and railways, several proactive roadbed cooling measures have been successfully applied on the QTP to maintain permafrost conditions and reduce the stress of permafrost thaw[23]. These measures include the installation of shading boards to control solar radiation, ventilation ducts, thermosiphons and air-cooled embankments to control heat convection, and crushed rock embankments to control heat conduction. For other building infrastructures, adaptation measures, such as the excavation of ice-rich ground, thermosiphons, and pile foundations, have been used to prevent the influence of thaw settlement and frost heave. The additional costs of adaptation measures were expressed as a proportion of replacement cost determined using the bill of quantities method according to a cost analysis of the designed adaptation measures. The cost assessment relied on an infrastructure database compiled for this study.

Infrastructure database. The infrastructure data included distribution, useful life, and replacement cost for roads, railways, powerlines, and buildings, which were collected from multiple sources. Road and railway distribution data were downloaded from the National Catalogue Service for the Geographic Information Website of China (www.webmap.cn). Data on buildings were derived from OpenStreetMap data (www.openstreetmap.org). The power line distribution source was from a predicted transmission line network dataset based on existing OpenStreetMap lines tagged in the 'source' column[52]. The useful life and replacement cost of infrastructure for cost impact analysis were obtained from Larsen et al. (2008)[27] but adjusted according to the design standards, project appraisal and budget documents of the engineering on the QTP, and personal communications with relevant employees and academic researchers studying the design and construction of infrastructure. The roads were further divided into five subtypes (four grades and one other subtype). Buildings were not further classified because of their low number and the dominance of residential buildings in the permafrost areas of the QTP. A total of 8 categories of infrastructure and their lifespans and replacement costs were used for impact analysis, including quantity and cost (Table 2).

Data availability

The authors declare that the data supporting the findings of this study are available within the paper, its supplementary information files, and the National Tibetan Plateau Data Center (https://doi.org/10.11888/Cryos.tpdc.272747).

Received: 16 March 2022; Accepted: 27 September 2022;
Published online: 13 October 2022

References

1. Melvin, A. M. et al. Climate change damages to Alaska public infrastructure and the economics of proactive adaptation. *Proc. Natl. Acad. Sci. USA* **114**, E122–E131 (2017).
2. Hjort, J. et al. Impacts of permafrost degradation on infrastructure. *Nat. Revi. Earth Environ.* **3**, 24–38 (2022).
3. Hjort, J. et al. Degrading permafrost puts Arctic infrastructure at risk by mid-century. *Nat. Commun.* **9**, 1–9 (2018).
4. Teufel, B. & Sushama, L. Abrupt changes across the Arctic permafrost region endanger northern development. *Nat. Clim. Chang.* **9**, 858–862 (2019).
5. Schneider von Deimling, T. et al. Consequences of permafrost degradation for Arctic infrastructure–bridging the model gap between regional and engineering scales. *Cryosphere* **15**, 2451–2471 (2021).
6. Rao, N. D., van Ruijven, B. J., Riahi, K. & Bosetti, V. Improving poverty and inequality modelling in climate research. *Nat. Clim. Chang.* **7**, 857–862 (2017).
7. Sun, M., Xu, X., Wang, L., Li, C. & Zhang, L. Stable energy, energy inequality, and climate change vulnerability in Pan-Third Pole regions: Empirical analysis in cross-national rural areas. Renew. *Sustain. Energy. Rev.* **147**, 111197 (2021).
8. Masson-Delmotte, V. et al. in *IPCC, 2021: Summary for Policymakers. In: Climate Change 2021: The Physical Science Basis. Contribution of Working Group I to the Sixth Assessment Report of the Intergovernmental Panel on Climate Change* (Cambridge Univ. Press, 2021).
9. Suter, L., Streletskiy, D. & Shiklomanov, N. Assessment of the cost of climate change impacts on critical infrastructure in the circumpolar Arctic. *Polar Geogr* **42**, 267–286 (2019).
10. Ran, Y. et al. New high-resolution estimates of the permafrost thermal state and hydrothermal conditions over the Northern Hemisphere. *Earth Syst. Sci. data* **14**, 865–884 (2022).
11. Wang, S., Niu, F., Chen, J. & Dong, Y. Permafrost research in China related to express highway construction. *Permafr. Periglac. Process.* **31**, 406–416 (2020).
12. Ran, Y. et al. Mapping the permafrost stability on the Tibetan Plateau for 2005–2015. *Sci. China Earth Sci* **64**, 62–79 (2021).
13. Yu, Q. et al. Analysis of tower foundation stability along the Qinghai–Tibet Power Transmission Line and impact of the route on the permafrost. *Cold Reg. Sci. Technol.* **121**, 205–213 (2016).
14. Ran, Y. et al. Biophysical permafrost map indicates ecosystem processes dominate permafrost stability in the Northern Hemisphere. *Environ. Res. Lett.* **16**, 095010 (2021).
15. Wester, P., Mishra, A., Mukherji, A. & Shrestha, A. B. *The Hindu Kush Himalaya Assessment—Mountains, Climate Change, Sustainability and People*. Springer Nature Switzerland AG, Cham, (2019).
16. Pepin, N. et al. Elevation-dependent warming in mountain regions of the world. *Nat. Clim. Chang.* **5**, 424–430 (2015).
17. You, Q. et al. Warming amplification over the Arctic Pole and Third Pole: Trends, mechanisms and consequences. *Earth-Science Reviews* **217**, 103625 (2021).
18. Nelson, F. E., Anisimov, O. A. & Shiklomanov, N. I. Subsidence risk from thawing permafrost. *Nature* **410**, 889–890 (2001).
19. Biskaborn, B. K. et al. Permafrost is warming at a global scale. *Nat. Commun.* **10**, 1–11 (2019).
20. Doré, G., Niu, F. & Brooks, H. Adaptation methods for transportation infrastructure built on degrading permafrost. *Permafr. Periglac. Process.* **27**, 352–364 (2016).
21. Zhao, R., Li, Z. W., Feng, G. C., Wang, Q. J. & Hu, J. Monitoring surface deformation over permafrost with an improved SBAS-InSAR algorithm: With emphasis on climatic factors modeling. *Remote Sens. Environ.* **184**, 276–287 (2016).
22. Cheng, G. A roadbed cooling approach for the construction of Qinghai–Tibet Railway. *Cold Reg. Sci. Technol.* **42**, 169–176 (2005).
23. Cheng, G., Sun, Z. & Niu, F. Application of the roadbed cooling approach in Qinghai–Tibet railway engineering. *Cold Reg. Sci. Technol.* **53**, 241–258 (2008).
24. Guo, L. et al. Displacements of tower foundations in permafrost regions along the Qinghai–Tibet Power Transmission Line. *Cold Reg. Sci. Technol.* **121**, 187–195 (2016).
25. Diaz, D. & Moore, F. Quantifying the economic risks of climate change. *Nat. Clim. Chang.* **7**, 774–782 (2017).
26. Wang, S. et al. The temporal effect of distress developments of frozen embankments in the permafrost regions along the Qinghai-Tibet Highway. *J. Test. Eval.* **47**, 3059–3079 (2018).
27. Larsen, P. H. et al. Estimating future costs for Alaska public infrastructure at risk from climate change. *Glob. Environ. Change* **18**, 442–457 (2008).
28. Bommer, C., Phillips, M. & Arenson, L. U. Practical recommendations for planning, constructing and maintaining infrastructure in mountain permafrost. *Permafr. Periglac. Process.* **21**, 97–104 (2010).
29. Schweikert, A., Espinet, X. & Chinowsky, P. The triple bottom line: bringing a sustainability framework to prioritize climate change investments for infrastructure planning. *Sustain. Sci.* **13**, 377–391 (2018).
30. Streletskiy, D. A., Suter, L. J., Shiklomanov, N. I., Porfiriev, B. N. & Eliseev, D. O. Assessment of climate change impacts on buildings, structures and infrastructure in the Russian regions on permafrost. *Environ. Res. Lett.* **14**, 025003 (2019).
31. Dore, M. H. I. & Burton, I. in *Costs of adaptation to climate change in Canada: A stratified estimate by sectors and regions: Social infrastructure*. (Brock Univ., 2001).
32. Porfiriev, B. N. et al. Climate change impact on economic growth and specific sectors' development of the Russian Arctic. *Arct. Ecol. Econ.* **28**, 4–17 (2017).
33. Porfiriev, B. N., Eliseev, D. O. & Streletskiy, D. A. Economic assessment of permafrost degradation effects on road infrastructure sustainability under climate change in the Russian Arctic. *Her. Russ. Acad. Sci.* **89**, 567–576 (2019).
34. Porfiriev, B. N., Elisseev, D. O. & Streletskiy, D. A. Economic Assessment of Permafrost Degradation Effects on the Housing Sector in the Russian Arctic. *Her.Russ. Acad. Sci.* **91**, 17–25 (2021).
35. Badina, S. V. Prediction of socioeconomic risks in the cryolithic zone of the Russian Arctic in the context of upcoming climate changes. *Stud. Russ. Econ. Dev.* **31**, 396–403 (2020).
36. Lu, P. et al. Lake outburst accelerated permafrost degradation on Qinghai-Tibet Plateau. *Remote Sens. Environ.* **249**, 112011 (2020).
37. Mekonnen, Z. A., Riley, W. J., Grant, R. F. & Romanovsky, V. E. Changes in precipitation and air temperature contribute comparably to permafrost degradation in a warmer climate. *Environ. Res. Lett.* **16**, 024008 (2021).
38. Reimchen, D., Stanley, B., Walsh, R., Doré, G. & Fortier, D. in *Reducing Maintenance Requirements on Permafrost-Affected Highways: Permafrost Test Sections Along the Alaska Highway, Yukon*. (In Proceedings of the XIII International Winter Road Congress, 2010).
39. You, Q. et al. Tibetan Plateau amplification of climate extremes under global warming of 1.5 °C, 2 °C and 3 °C. *Glob. Planet. Chang.* **192**, 103261 (2020).
40. Nicolsky, D. J., Romanovsky, V. E., Panda, S. K., Marchenko, S. S. & Muskett, R. R. Applicability of the ecosystem type approach to model permafrost dynamics across the Alaska North Slope. *J. Geophys. Res-Earth Surface* **122**, 50–75 (2017).
41. Devoie, E. G., Craig, J. R., Connon, R. F. & Quinton, W. L. Taliks: A Tipping Point in Discontinuous Permafrost Degradation in Peatlands. *Water Resources Res.* **55**, 9838–9857 (2019).
42. Fick, S. E. & Hijmans, R. J. WorldClim 2: new 1-km spatial resolution climate surfaces for global land areas. *Int. J. Climatol.* **37**, 4302–4315 (2017).
43. Zhang, T. et al. Spatial and temporal variability in active layer thickness over the Russian Arctic drainage basin. *J. Geophys. Res. Atmos.* **110,** 5642 (2005).
44. Aalto, J., Karjalainen, O., Hjort, J. & Luoto, M. Statistical forecasting of current and future circum-Arctic ground temperatures and active layer thickness. *Geophys. Res. Lett.* **45**, 4889–4898 (2018).
45. Wang, Y. et al. Tens of thousands additional deaths annually in cities of China between 1.5 C and 2.0 C warming. *Nat. Commun.* **10**, 1–7 (2019).
46. Hengl, T. et al. SoilGrids250m: Global gridded soil information based on machine learning. *PLoS One* **12**, e0169748 (2017).
47. Xu, X. M. & Wu, Q. B. Impact of climate change on allowable bearing capacity on the Qinghai-Tibetan Plateau. *Adv. Clim. Chang. Res.* **10**, 99–108 (2019).
48. Streletskiy, D. A., Shiklomanov, N. I. & Nelson, F. E. Permafrost, infrastructure, and climate change: a GIS-based landscape approach to geotechnical modeling. *Arct. Antarct. Alp. Res.* **44**, 368–380 (2012).
49. Cheng, G. et al. Characteristic, changes and impacts of permafrost on Qinghai-Tibet Plateau. *Chin. Sci. Bull.* **64**, 2783–2795 (2019).
50. Scripter, M. W. Nested-means map classes for statistical maps. *Ann. Assoc. Am. Geog.* **60**, 385–392 (1970).
51. Daanen, R. P. et al. Permafrost degradation risk zone assessment using simulation models. *Cryosphere* **5**, 1043–1056 (2011).
52. Arderne, C., Zorn, C., Nicolas, C. & Koks, E. E. Predictive mapping of the global power system using open data. *Sci. data* **7**, 1–12 (2020).

Acknowledgements

This study was jointly supported by the Strategic Priority Research Program of the Chinese Academy of Sciences (grant number XDA19070204) and the National Natural Science Foundation of China projects (grant numbers 42071421). JH received funding from the Academy of Finland (grant number 315519). We thank Dr. Defu Zou and Dr. Qiangqiang Pang for providing ground ice content data for the QTP. The authors also

thank the associate editor and three anonymous reviewers for their insightful comments and suggestions that helped improve this paper.

Author contributions

Y.R. and G.C. designed the study. Y.R., Y.D., and M.T. prepared the datasets and ran the model. Y.R. and X.L. performed the analyses. Y.R., X.L. and J.H. drafted the manuscript. G.C., X.L., J.H., L.L. and S.K. provided advice, ideas, and discussion and improved the writing and structure of the paper.

Competing interests

The authors declare no competing interests.

Additional information

Supplementary information The online version contains supplementary material available at https://doi.org/10.1038/s43247-022-00568-6.

Correspondence and requests for materials should be addressed to Youhua Ran.

Peer review information *Communications Earth & Environment* thanks the anonymous reviewers for their contribution to the peer review of this work. Primary Handling Editors: Olga Churakova and Joe Aslin.